Transient Vibration Prediction for Rotors on Ball Bearings Using Load-Dependent Non-Linear Bearing Stiffness

David P. Fleming
Glenn Research Center, Cleveland, Ohio

J.V. Poplawski
J.V. Poplawski and Associates, Bethlehem, Pennsylvania

The NASA STI Program Office . . . in Profile

Since its founding, NASA has been dedicated to the advancement of aeronautics and space science. The NASA Scientific and Technical Information (STI) Program Office plays a key part in helping NASA maintain this important role.

The NASA STI Program Office is operated by Langley Research Center, the Lead Center for NASA's scientific and technical information. The NASA STI Program Office provides access to the NASA STI Database, the largest collection of aeronautical and space science STI in the world. The Program Office is also NASA's institutional mechanism for disseminating the results of its research and development activities. These results are published by NASA in the NASA STI Report Series, which includes the following report types:

- TECHNICAL PUBLICATION. Reports of completed research or a major significant phase of research that present the results of NASA programs and include extensive data or theoretical analysis. Includes compilations of significant scientific and technical data and information deemed to be of continuing reference value. NASA's counterpart of peer-reviewed formal professional papers but has less stringent limitations on manuscript length and extent of graphic presentations.

- TECHNICAL MEMORANDUM. Scientific and technical findings that are preliminary or of specialized interest, e.g., quick release reports, working papers, and bibliographies that contain minimal annotation. Does not contain extensive analysis.

- CONTRACTOR REPORT. Scientific and technical findings by NASA-sponsored contractors and grantees.

- CONFERENCE PUBLICATION. Collected papers from scientific and technical conferences, symposia, seminars, or other meetings sponsored or cosponsored by NASA.

- SPECIAL PUBLICATION. Scientific, technical, or historical information from NASA programs, projects, and missions, often concerned with subjects having substantial public interest.

- TECHNICAL TRANSLATION. English-language translations of foreign scientific and technical material pertinent to NASA's mission.

Specialized services that complement the STI Program Office's diverse offerings include creating custom thesauri, building customized data bases, organizing and publishing research results . . . even providing videos.

For more information about the NASA STI Program Office, see the following:

- Access the NASA STI Program Home Page at *http://www.sti.nasa.gov*

- E-mail your question via the Internet to help@sti.nasa.gov

- Fax your question to the NASA Access Help Desk at 301–621–0134

- Telephone the NASA Access Help Desk at 301–621–0390

- Write to:
  NASA Access Help Desk
  NASA Center for AeroSpace Information
  7121 Standard Drive
  Hanover, MD 21076

NASA/TM—2002-211829

Transient Vibration Prediction for Rotors on
Ball Bearings Using Load-Dependent
Non-Linear Bearing Stiffness

David P. Fleming
Glenn Research Center, Cleveland, Ohio

J.V. Poplawski
J.V. Poplawski and Associates, Bethlehem, Pennsylvania

National Aeronautics and
Space Administration

Glenn Research Center

August 2002

Available from

Transient Vibration Prediction for Rotors on Ball Bearings Using Load-Dependent Non-Linear Bearing Stiffness

David P. Fleming
National Aeronautics and Space Administration
Glenn Research Center
Cleveland, Ohio

J.V. Poplawski
J.V. Poplawski and Associates
Bethlehem, Pennsylvania

Abstract

Rolling-element bearing forces vary nonlinearly with bearing deflection. Thus an accurate rotordynamic transient analysis requires bearing forces to be determined at each step of the transient solution. Analyses have been carried out to show the effect of accurate bearing transient forces (accounting for non-linear speed and load dependent bearing stiffness) as compared to conventional use of average rolling-element bearing stiffness. Bearing forces were calculated by COBRA-AHS (Computer Optimized Ball and Roller Bearing Analysis - Advanced High Speed) and supplied to the rotordynamics code ARDS (Analysis of RotorDynamic Systems) for accurate simulation of rotor transient behavior. COBRA-AHS is a fast-running 5 degree-of-freedom computer code able to calculate high speed rolling-element bearing load-displacement data for radial and angular contact ball bearings and also for cylindrical and tapered roller bearings. Results show that use of nonlinear bearing characteristics is essential for accurate prediction of rotordynamic behavior.

Introduction

Rotordynamics analyses are now fairly mature, yielding accurate predictions of rotor behavior as long as the input data are accurate. Modern codes can almost universally be run on personal computers, making them very portable; an example is ARDS [1, 2]. The challenge nowadays is to furnish the rotordynamics code with accurate input data such as bearing stiffness.

Response of all but very flexible rotors depends strongly on bearing properties. When bearings are nonlinear, accurate rotor response calculations demand use of bearing properties for the precise conditions encountered, rather than average properties. Fluid film bearings have been studied for over 100 years and their properties can be calculated fairly well; moreover, for many uses these bearings behave in a reasonably linear manner. Rolling-element bearings, on the other hand, not only have a somewhat shorter analytical history, but also have a much less linear force-displacement relationship.

Analyses of load-stress relationships for rolling element bearings were published by Lundberg and Palmgren in the 1940s [3]. These relationships were not easily usable until the analytical additions of Jones [4] led to the marketing of his computer code in the 1960s. Jones' code, which is still the most widely used rolling-element bearing analysis tool, is primarily for calculation of bearing stress and fatigue

life, with load-deflection data only a byproduct. The code COBRA-AHS (Computer Optimized Ball and Roller Bearing Analysis—Advanced High Speed) has been developed recently under a NASA Small Business Innovative Research (SBIR) contract [5]. COBRA-AHS is intended to be a major improvement over earlier rolling-element bearing analytical tools; use of up-to-date stress/life data, accurate stress calculations considering bearing installation press fits, and an interactive front end are some of its characteristics. It accounts for 5 degrees of freedom in the bearing, and can calculate load-displacement data for high speed radial and angular contact ball bearings and also for cylindrical and tapered roller bearings. It executes rapidly; thus it was natural to consider making it callable by a rotordynamics code for accurate transient calculations. The rotordynamics code chosen is ARDS (Analysis of RotorDynamic Systems) [1, 2], a versatile public-domain code.

Analytical System and Procedure

Figure 1 is an ARDS drawing of the shaft system. It depicts a fairly stiff shaft with concentrated masses (which may represent compressor or turbine wheels) at stations 3 and 4. In total, 6 stations and 5 elements were used in the model, with 3 of the elements made up of 2 or more subelements.
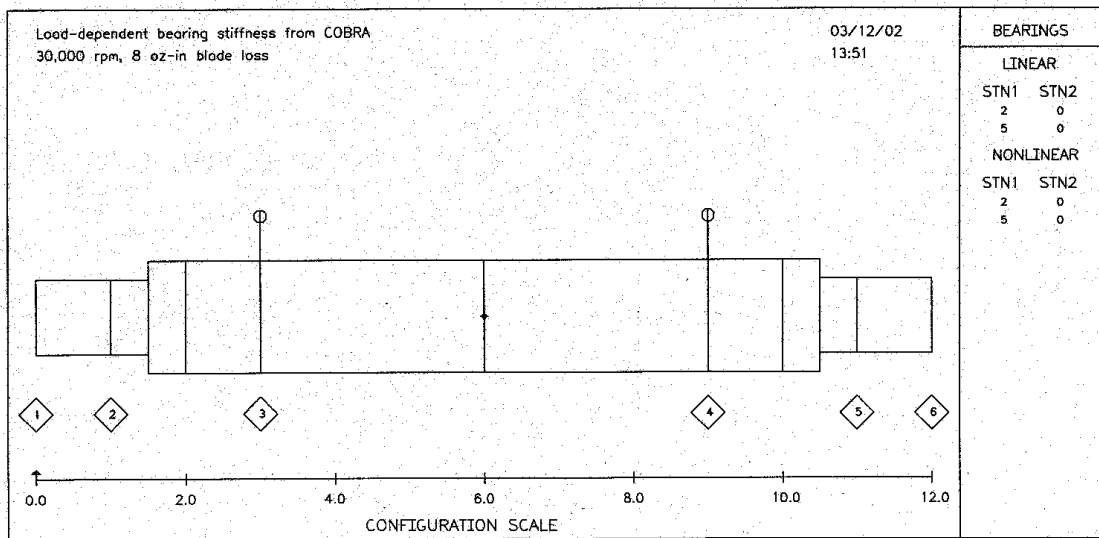

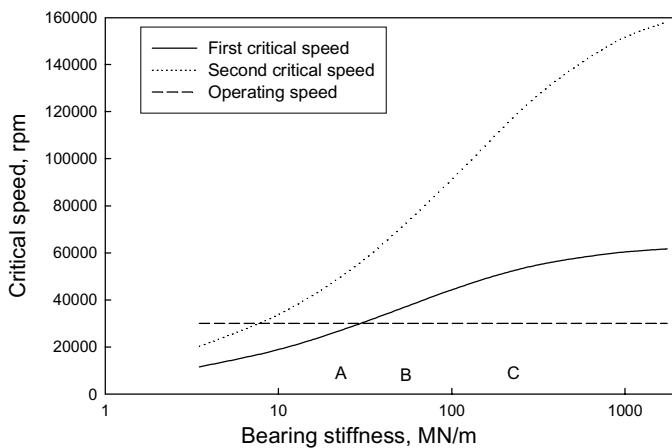**Figure 1. ARDS drawing of rotor**

Figure 2. Critical speeds for varying bearing stiffness

Radial (deep groove) ball bearings of 25 mm bore diameter are at stations 2 and 5. The shaft material is steel; total mass of the shaft system is 4.6 kg.

Figure 2 shows the first two system critical speeds as a function of bearing stiffness. Letters *A, B,* and *C* denote specific stiffness values to be discussed later. For stiffness up to about 200 MN/m (approximately at point *C*), critical speeds rise rapidly with stiffness, indicating significant bearing participation in the rotor motion. Above 200 MN/m, critical speeds do not increase as rapidly, indicating that

increasing amounts of motion are due to shaft bending rather than bearing deflection. Mode shapes calculated at critical speeds, shown in figure 3 for two values of bearing stiffness, confirm this. For a bearing stiffness of 18 MN/m, most of the elastic deflection takes place in the bearings. At the higher stiffness of 180 MN/m, on the other hand, nearly all of the elastic deflection is in the shaft at the first critical speed, while at the second critical speed deflection is about evenly divided between bearings and shaft.
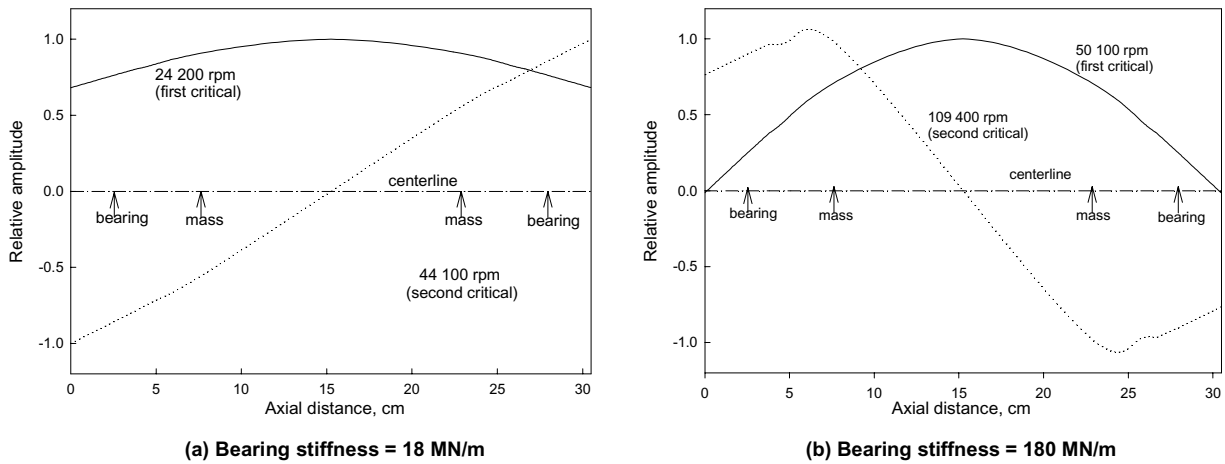

(a) Bearing stiffness = 18 MN/m

(b) Bearing stiffness = 180 MN/m

Figure 3. Critical speed mode shapes

Shaft transient response to suddenly applied imbalance was studied at 30000 rpm. The imbalance magnitudes were those that could have resulted from loss of a blade in a turbomachine. COBRA-AHS could have been called at each time step of the analysis to supply bearing force at the current displacement. However, for the present studies with only one bearing variable (radial displacement; speed is constant) it was more efficient to run COBRA-AHS once to generate load versus deflection data for the bearings. A fourth-order curve was then fitted to these data and the coefficients supplied to ARDS. Figure 4 shows two stiffness curves from the bearing data. The upper curve is the incremental stiffness, that is, the slope

Figure 4. Ball bearing stiffness

of the load-deflection curve. This stiffness would be used if one were studying motion about an off-center steady-state point. The lower curve is the load divided by the deflection, or average stiffness; it is this value that was used by ARDS for calculation of the instantaneous bearing force. Note that, for both curves, there is more than an order of magnitude increase over the range of the figure. This illustrates the significant nonlinearity of the ball bearing used, and is representative of rolling-element bearings.
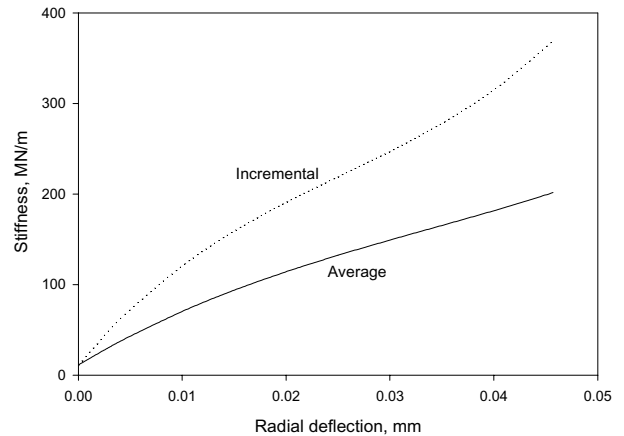
For the low deflection expected at normal (well-balanced) operating conditions, the bearing stiffness is about 20 MN/m. Reference to figure 2 (stiffness point *A*) shows that this places the initial operating condition between the first and second critical speeds. For higher stiffness resulting from higher bearing loads due to rotor imbalance, the operating regime of the rotor could well change to subcritical. Thus, as will be seen, having accurate bearing characteristics for the particular operating condition is vital for prediction of rotor behavior.

Results

Transient orbit plots for suddenly applied imbalances of 36, 144, and 576 g cm and a speed of 30 000 rpm are shown as figure 5 using the ball bearing properties calculated by COBRA-AHS. The imbalance was applied at station 4 (the location of one of the concentrated masses), and the orbits are those of station 5, the right bearing location. One hundred time steps per revolution were used by the transient analysis, and five revolutions are plotted. The plotting code superimposes a small circle on the orbit trace at the completion of each revolution; these are numbered 1 through 5 in the plots. The leftmost plot, for 36 g cm imbalance, shows the amplitude increasing more or less smoothly to its steady-state value of 9 μm, with only a small overshoot. In the middle plot, for 144 g cm imbalance, the orbit is not as smooth, and the amplitude of 18 μm at the end of five revolutions is noticeably less than the maximum of 23 μm seen in the plot. The rightmost plot, for 576 g cm imbalance, is somewhat more ragged looking, and again the maximum amplitude reached, 49 μm, is greater than the 39 μm seen at the end of five revolutions. The amount by which the amplitude overshoots the steady-state value depends on bearing damping. While damping in rolling-element bearings is known to be low, precise values are not readily available. A value of 2 kN/m was used in the analyses; this is close to the estimates reported in [6].
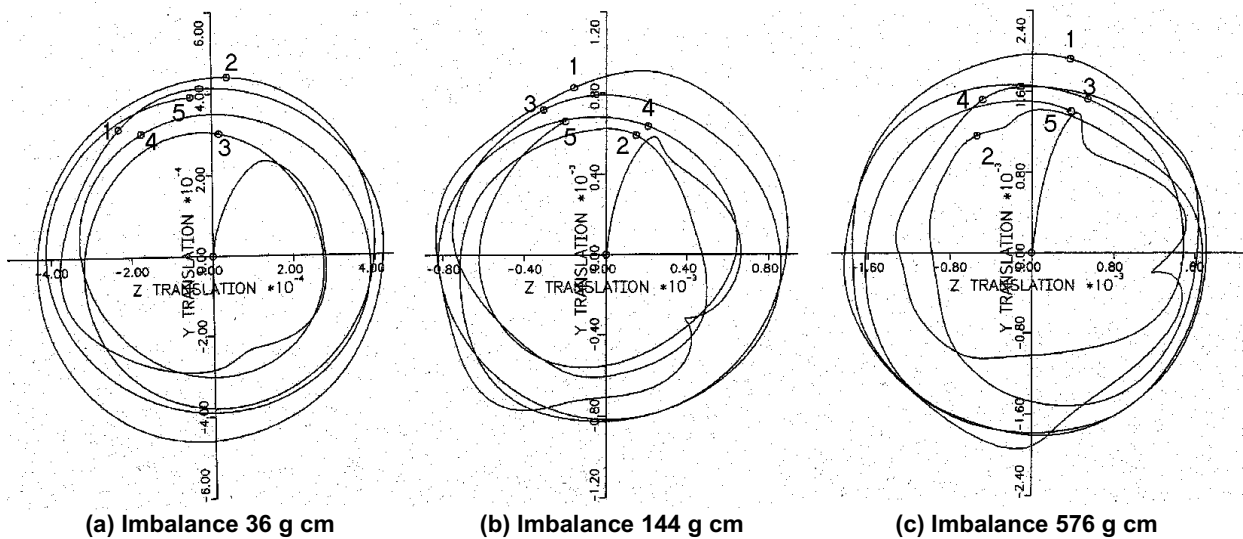

(a) Imbalance 36 g cm   (b) Imbalance 144 g cm   (c) Imbalance 576 g cm

Figure 5. Transient orbits for load-dependent bearing stiffness

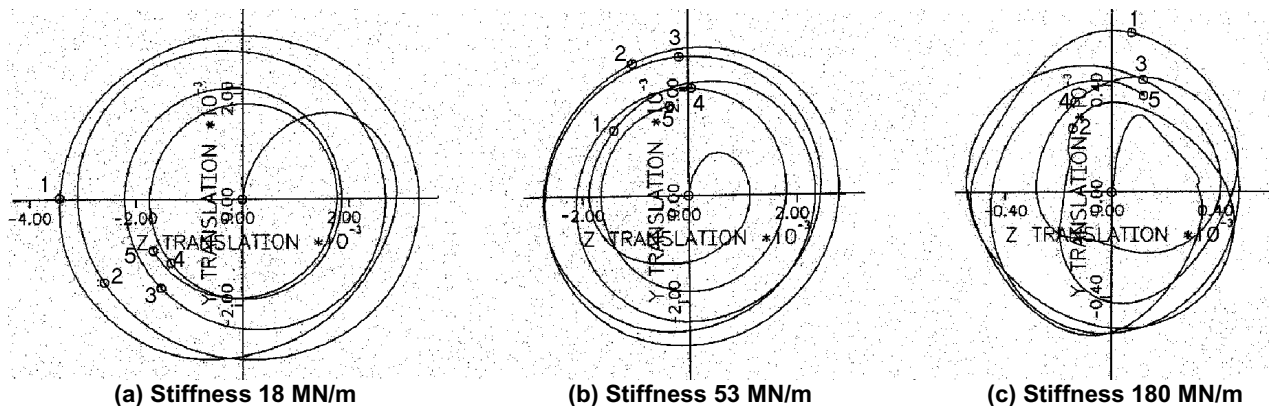(a) Stiffness 18 MN/m   (b) Stiffness 53 MN/m   (c) Stiffness 180 MN/m

Figure 6. Transient orbits for constant bearing stiffness. Imbalance 144 g cm

Parts a, b, and c of figure 5 each use different scales, namely 5, 10, and 20 microns per division (0.0002, 0.0004, and 0.0008 inches per division); thus the orbit sizes are roughly in the ratio of 1, 2, and 4. However, the imbalances are in the ratio 1, 4, and 16; thus the orbit size for these three cases is roughly proportional to the square root of the imbalance. This is not a surprising result, since the bearing stiffness increases with the load applied.

For comparison, orbit plots for three values of linear bearing stiffness (18, 53, and 180 MN/m) and an imbalance of 144 g cm are shown as figure 6. Again, numbers are placed on the plots denoting the number of completed revolutions. For these cases it suffices to consider only one level of imbalance, since, for linear bearings, amplitudes are directly proportional to imbalance. The left and center orbits are fairly smooth, and all the orbits show a maximum amplitude that is significantly larger than the amplitude at the end of 5 revolutions. Reference to figure 2 (stiffness point *A*) shows that the operating condition for the left plot is between the first and second critical speeds, while for the center and right plots (corresponding to points *B* and *C* in fig. 2) operation is entirely subcritical. Surprisingly, the left and center orbits (plotted to the same scale of 50 μm (0.002 in) per division) are nearly the same size, and much larger than the orbit of figure 5(b) for the same imbalance. However, the right orbit (plotted at a magnified scale of 10 μm (0.0004 in) per division) is much smaller. One may reasonably conclude from figures 5 and 6 that estimation of average linear bearing stiffness, and consequently accurate rotordynamic prediction with a linear analysis, is difficult at best.

ARDS was allowed to run for a longer time (40 revolutions) in order to discern the steady state that would be attained following the imposition of imbalance. Figure 7 summarizes the results, obtained from measurements on the orbit plots made using variable bearing stiffness from COBRA-AHS. As seen previously from the orbits (fig. 5), shaft peak amplitude is higher than the eventual steady state value.
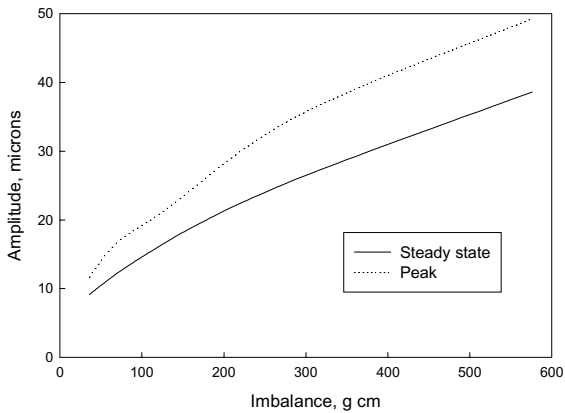

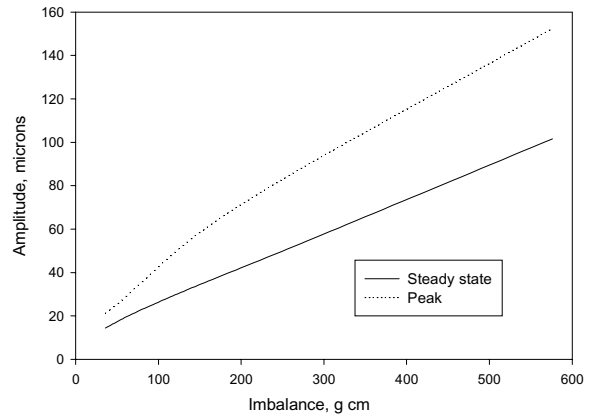Figure 7. Station 5 amplitude after sudden imbalance

Figure 8. Station 4 amplitude after sudden imbalance

Figure 8 displays the amplitude at station 4, the location of the imbalance. The trend as imbalance changes is similar to figure 7, but the amplitudes are larger, and they increase at a greater rate than do amplitudes at the bearings. Figure 9 shows the reason for this. This figure shows the mode shape assumed by the rotor as the motion approaches steady state. Even though the rotor speed is well below the critical speeds calculated for the effective bearing stiffness, there is significant rotor bending. The rotor bending causes vibration amplitude to be considerably larger over the rotor midspan than at the bearings. Moreover, the amount of bending increases with imbalance, producing a greater disparity between bearing and midspan amplitudes.

Figure 10 plots the effective stiffness of the bearing at station 5 for the range of imbalance studied; it is calculated as the bearing load divided by the vibration amplitude. The stiffness curve labeled *peak* is naturally higher than that for steady state because of the higher peak amplitude. Both peak and steady-state stiffness increase with the amount of imbalance, again because of the corresponding higher amplitudes.

The effective stiffness of 170 MN/m for steady state conditions with 576 g cm imbalance is close to the stiffness of 180 MN/m used for figure 3 (b). There is a similarity in mode shapes between figures 3(b) and 9, with the shape of figure 9 being that of the first mode of fig. 3 (b) modified by the second mode. This similarity of mode shapes occurs despite the operating speed of 30 000 rpm being well below the first critical speed of 50 100 rpm shown in figure 3(b). This implies that the observed mode will correspond to the critical speed mode shapes for the effective bearing stiffness, even if the operating speed is well removed from the critical speed. A further implication is that the bearing stiffness of significance is that at the operating condition; this stiffness may be considerably different than at design condition. Furthermore, identical bearings at different locations on the rotor may have different stiffnesses, as determined by the bearing deflection; note, from figure 9, that the amplitudes are not the same at the two bearing locations. The imbalance was applied closer to the right-hand bearing, leading to greater amplitude on the right side of the rotor.
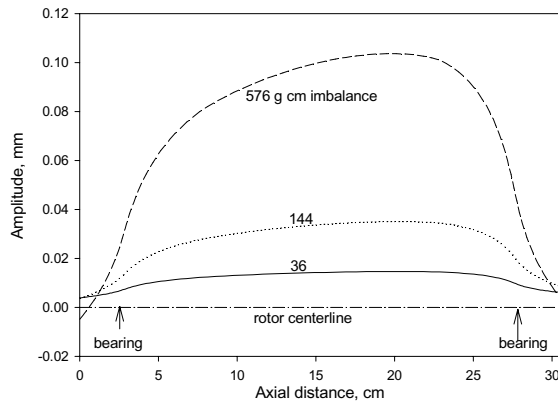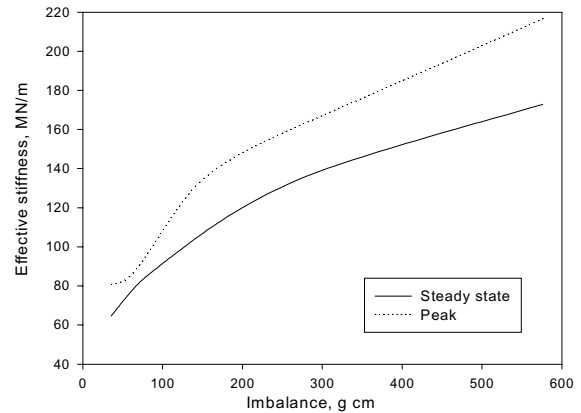

Figure 9. Rotor steady state mode shapes

Figure 10. Station 5 effective bearing stiffness

Concluding Remarks

Transient rotordynamic calculations were made for suddenly applied imbalance on a ball bearing supported rotor. Accurate bearing forces were obtained at each time step from data generated by COBRA-AHS. For the bearings employed, effective bearing stiffness increased substantially with bearing deflection. As a result, bearing vibration increased less than linearly with the amount of imbalance. Vibration amplitude at rotor midspan was larger than at the bearings because of rotor bending, but again the rate of vibration increase with imbalance was less than linear. The rotor assumed a mode shape corresponding to the critical speed mode shapes, even though the operating speed was well removed from any critical speed. Results show that it is essential to use amplitude-dependent bearing properties in order to obtain accurate rotordynamic predictions.

References

1. Nelson, H.D.; Meacham, W.L.; Fleming, D.P.; and Kascak, A.F. (1983): Nonlinear Analysis of Rotor-Bearing Systems Using Component Mode Synthesis. *Journal of Engineering for Power*, vol. 105, no. 3, pp. 606–614.

2. Fleming, David P. (1996): Rotordynamics on the PC: Transient Analysis with ARDS. *Rotating Machinery—1996* (Proceedings of the Sixth International Symposium on Transport Phenomena and Dynamics of Rotating Machinery), Vol. I, D.C. Han, S.T. Ro, and J.H. Kim, eds., Pacific Center of Thermal-Fluids Engineering, Kihei, Maui, Hawaii, U.S.A., pp. 367–375.

3. Lundberg, G., and Palmgren, A. (1947): Dynamic Capacity of Rolling Bearings. *Acta Polytechnica* (Mechanical Engineering Series), vol. I, no. 3.

4. Jones, A.B. (1960): A General Theory for Elastically Constrained Ball and Radial Roller Bearings Under Arbitrary Load and Speed Conditions. *Trans. ASME, J. Basic Eng.*, vol. 82, no. 2, pp. 309–320.

5. Poplawski, J.V.; Rumbarger, J.H.; Peters, S.M.; Flower, R.; and Galaitis, H. (2002): Advanced Analysis Package for High Speed Multi-Bearing Shaft Systems: COBRA-AHS. Final Report, NASA Contract NAS3–00018.

6. Lewis, P.; and Malanoski, S.B. (1965): Rotor-Bearing Dynamics Design Technology; Part IV: Ball Bearing Design Data. AFAPL-TR-65-45, Part IV.

REPORT DOCUMENTATION PAGE

Public reporting burden for this collection of information is estimated to average 1 hour per response, including the time for reviewing instructions, searching existing data sources, gathering and maintaining the data needed, and completing and reviewing the collection of information. Send comments regarding this burden estimate or any other aspect of this collection of information, including suggestions for reducing this burden, to Washington Headquarters Services, Directorate for Information Operations and Reports, 1215 Jefferson Davis Highway, Suite 1204, Arlington, VA 22202-4302, and to the Office of Management and Budget, Paperwork Reduction Project (0704-0188), Washington, DC 20503.

1. AGENCY USE ONLY (Leave blank)	2. REPORT DATE	3. REPORT TYPE AND DATES COVERED
	August 2002	Technical Memorandum

4. TITLE AND SUBTITLE

Transient Vibration Prediction for Rotors on Ball Bearings Using
Load-Dependent Non-Linear Bearing Stiffness

5. FUNDING NUMBERS

WU–728–30–10–00

6. AUTHOR(S)

David P. Fleming and J.V. Poplawski

7. PERFORMING ORGANIZATION NAME(S) AND ADDRESS(ES)

National Aeronautics and Space Administration
John H. Glenn Research Center at Lewis Field
Cleveland, Ohio 44135–3191

8. PERFORMING ORGANIZATION REPORT NUMBER

E–13523

9. SPONSORING/MONITORING AGENCY NAME(S) AND ADDRESS(ES)

National Aeronautics and Space Administration
Washington, DC 20546–0001

10. SPONSORING/MONITORING AGENCY REPORT NUMBER

NASA TM—2002-211829

11. SUPPLEMENTARY NOTES

Prepared for the IFToMM Sixth International Conference on Rotor Dynamics sponsored by the National Committee of Applied Mechanics of The Institution of Engineers, Sydney, Australia, September 30–October 3, 2002. David P. Fleming, NASA Glenn Research Center, and J.V. Poplawski, J.V. Poplawski and Associates, Bethlehem, Pennsylvania. Responsible person, David P. Fleming, organization code 5950, 216–433–6013.

12a. DISTRIBUTION/AVAILABILITY STATEMENT

Unclassified - Unlimited
Subject Category: 37   Distribution: Nonstandard

Available electronically at http://gltrs.grc.nasa.gov

This publication is available from the NASA Center for AeroSpace Information, 301–621–0390.

12b. DISTRIBUTION CODE

13. ABSTRACT *(Maximum 200 words)*

Rolling-element bearing forces vary nonlinearly with bearing deflection. Thus an accurate rotordynamic transient analysis requires bearing forces to be determined at each step of the transient solution. Analyses have been carried out to show the effect of accurate bearing transient forces (accounting for non-linear speed and load dependent bearing stiffness) as compared to conventional use of average rolling-element bearing stiffness. Bearing forces were calculated by COBRA-AHS (Computer Optimized Ball and Roller Bearing Analysis - Advanced High Speed) and supplied to the rotordynamics code ARDS (Analysis of Rotor Dynamic Systems) for accurate simulation of rotor transient behavior. COBRA-AHS is a fast-running 5 degree-of-freedom computer code able to calculate high speed rolling-element bearing load-displacement data for radial and angular contact ball bearings and also for cylindrical and tapered roller bearings. Results show that use of nonlinear bearing characteristics is essential for accurate prediction of rotordynamic behavior.

14. SUBJECT TERMS

Rotordynamics; Rolling-element bearing stiffness; Transient dynamic analysis;
Rolling-element bearings; Bearing life

15. NUMBER OF PAGES

13

16. PRICE CODE

17. SECURITY CLASSIFICATION OF REPORT	18. SECURITY CLASSIFICATION OF THIS PAGE	19. SECURITY CLASSIFICATION OF ABSTRACT	20. LIMITATION OF ABSTRACT
Unclassified	Unclassified	Unclassified	